Chemical Physics 368 (2010) 62–65

Contents lists available at ScienceDirect

Chemical Physics

journal homepage: www.elsevier.com/locate/chemphys

The nature of intramolecular hydrogen bond in 2-nitromalonaldehyde

Sayyed Faramarz Tayyari [a,*], Mansoureh Zahedi-Tabrizi [b], Hossein Azizi-Toupkanloo [a], Steven S. Hepperle [c], Yan Alexander Wang [c,*]

[a] Department of Chemistry, Ferdowsi University of Mashhad, Mashhad 91775-1436, Iran
[b] Department of Chemistry, University of Alzahra, Tehran, Iran
[c] Department of Chemistry, University of British Columbia, Vancouver, Canada BC V6T 1Z1

ARTICLE INFO

Article history:
Received 6 June 2009
In final form 11 December 2009
Available online 16 December 2009

Keywords:
Two dimensional double minimum potential
2-Nitromalonaldehyde
Proton tunneling
Tunneling frequency
Barrier height

ABSTRACT

A simple, practical method for treating the proton tunneling in 2-nitromalonaldehyde (NO_2MA) was used. A two-dimensional potential energy surface (PES) function, which couples OH stretching and in-plane bending modes, has been constructed for motions of the hydrogen atom by the aid of quantum mechanical calculations at the MP2/6-31G** level for a fixed skeleton geometry. This PES function was used to calculate energy levels, from which a tunneling splitting of 34.5 and 3.2 cm^{-1} was obtained for light and deuterated NO_2MA, respectively, in excellent agreement with the experimental value of 35.0 ± 15.0 and 3.0 ± 0.02 cm^{-1}, respectively. The double-well barrier height was predicted to be 46.4 kJ/mol with respect to the midpoint between the two adjacent minima of the hydrogen motions on the PES. The hydrogen-bond strength was estimated to be over 50 kJ/mol.

1. Introduction

For a long time, hydrogen bond and proton transfer have been used to explain diverse chemical, biological, and physical phenomena [1–4]; yet, important questions regarding their origin and manifestation continue to emerge. Proton transfer reactions and hydrogen bonds are ubiquitous and of fundamental importance to many chemical and most biological systems, where proton transfer inter-converts different structures of possible tautomers of a molecule.

To treat proton tunneling in bent hydrogen-bonded systems, we have developed a simple method, in which a two-dimensional potential energy surface (PES) function was able to describe the motion of the hydrogen atom successfully [5,6]. Based on quantum mechanical calculations, this PES function was designed to couple O–H stretching and in-plane bending modes of the hydrogen-bond proton potential in the malonaldehyde (MA) [5] and 6-hydroxy-2-formylfulvene (HFF) [6] systems.

To further test its effectiveness, we now apply this simple method to study the proton potential function in 2-nitromalonaldehyde (NO_2MA), a β-dicarbonyl compound prominently in the *cis*-enol form (Fig. 1), whose structure and vibrational spectra of NO_2MA were recently discussed [7]. Using a coupled Hamiltonian for the two lowest states of the deuterated NO_2MA, Caminati was able to determine the energy separation between these two states (ΔE_{01}) to be 3.00 ± 0.02 cm^{-1}, whereas the counterpart was found to be nearly a dozen times bigger (35.0 ± 15.0 cm^{-1}) for the undeuterated NO_2MA based on relative intensity measurements [8]. Judging from the corresponding values for the undeuterated and deuterated malonaldehyde (21.5 and 2.88 cm^{-1}, respectively), we also expect a tunneling frequency slightly above 21.5 cm^{-1} for the normal (undeuterated) NO_2MA.

In the following, we will assess the performance of our simple method in predicting the proton tunneling, O–H/O–D stretching and in-plane bending frequencies for NO_2MA.

2. Computational procedure

All *ab initio* calculations in this work were performed using the Gaussian 03W [9] and DBMIN2 [10] programs. The structure of NO_2MA was fully optimized at the MP2 level using the 6-31G** basis set and at the B3LYP level using the 6-31G**, 6-311G**, and 6-311++G** basis sets. To compare the hydrogen-bond strength in NO_2MA with that in MA, the open structures with 180° rotation of the O–H bond (Fig. 1b) of both molecules were also fully optimized at the B3LYP level using the aforementioned basis sets.

To explore two-dimensional proton tunneling, we varied the O–H distance in NO_2MA from 0.8 Å to the midpoint between the two minima and the COH angle from 90° to 120°, and calculated the energies at the MP2/6-31G** and MP4/6-31G** levels by fixing

* Corresponding authors. Tel.: +98 511 8780216; fax: +98 511 8438032 (S.F. Tayyari).
E-mail addresses: Tayyari@ferdowsi.um.ac.ir (S.F. Tayyari), yawing@zodiac.chem.ubc.ca (Y.A. Wang).

0301-0104/$ - see front matter © 2009 Elsevier B.V. All rights reserved.
doi:10.1016/j.chemphys.2009.12.016

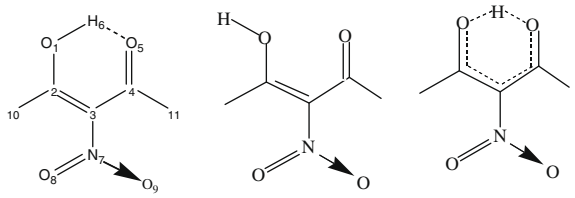

Fig. 1. Schematic representation of NO_2MA in (a) the *cis*-enol, (b) the *trans*-enol, and (c) the C_{2v} forms.

all other parameters at their optimized equilibrium values obtained at MP2/6-31G**. The potential energy surfaces obtained at these levels were fitted nonlinearly to the following two-dimensional anharmonic potential function:

$$V = 1/2[K_s X^2 + K_{ss} X^4 + K_b Y^2 + K_{ssb} X^2 Y] \quad (1)$$

using the Genplot package [11], where K_s and K_{ss} represent the quadratic and quartic force constants in the X (stretching) direction, respectively, K_b represents the quadratic force constant in the Y (bending) direction, and K_{ssb} represents the interaction between the stretching and bending modes. Inclusion of other terms, such as X^6, Y^3, X^2Y^2, and X^2Y^3, did not improve the fitting and thus they were not used.

To benchmark the barrier height calculated from Eq. (1) against that on the potential energy surface with full relaxed geometries, the energy of the C_{2v} transition state (Fig. 1c), in which the proton is in the midway of the two O atoms, was also computed. The energy difference between this C_{2v} structure and the energy minimal position (Fig. 1a) is denoted as E_{BH}, referring to the barrier height obtained from fully relaxed potential energy surface.

2.1. Hamiltonian

The above symmetric double minimum potential function, Eq. (1), was then introduced into a Hamiltonian for a bent triatomic system,

$$\hat{H} = 1/2\left[K_s \mu Q_s^2 + K_{ss}\mu^2 Q_s^4 + K_b \mu Q_b^2 + K_{ssb}\mu^{1.5} Q_s^2 Q_b + P_s^2 + P_b^2\right], \quad (2)$$

where Q_s and Q_b are mass weighted coordinates in the stretching (X) and bending (Y) directions, respectively, μ is the reduced mass of the system (simply the O–H/O–D group), and P_s and P_b are the corresponding momenta. It is noteworthy that our values for μ are the same as those used by Bevan [12] (0.94809 and 1.78885 a.u. for O–H and O–D, respectively). Moreover, our μ values are not very different from those calculated by Matanović and Došlić [13]: 0.928 a.u. at the equilibrium geometry and slightly different, 0.932 a.u., at the saddle point for the undeuterated acetylacetone. Taking the suggestions of Ibres [14] and by Singh and Wood [15], we did not incorporate possible interaction with the O···O stretching in the above Hamiltonian, Eq. (2). The accuracy of the computational results presented below will justify this simplified approach.

The corresponding wave function could be expressed in terms of binary products of the orthonormal harmonic oscillator wave functions:

$$\psi_r = \sum_i \sum_j a_{ij}^r \Phi_i(Q_s)\Phi_j(Q_b). \quad (3)$$

where $\left\{a_{ij}^r\right\}$ are the wave function expansion coefficients and the upper limits of the summation indexes $i = 0, 1, 2, \ldots, N_s$ and $j = 0, 1, 2, \ldots, N_b$, respectively. Substituting Eq. (3) into the Schrödinger equation $\hat{H}\psi_r = E\psi_r$, multiplying both sides by $\Phi_k^*(Q_s)\Phi_l^*(Q_b)$, and integrating over Q_s and Q_b, we have

$$\sum_i \sum_j a_{ij}^r H_{kl,ij} = E_{ra_{kl}}^r, \quad (4)$$

where,

$$H_{kl,ij} = \int_{-\infty}^{+\infty} \Phi_k^*(Q_s)\Phi_l^*(Q_b)\hat{H}\Phi_i(Q_s)\Phi_j(Q_b)dQ_s dQ_b = \langle k,l|\hat{H}|i,j\rangle$$

Rearrangement of Eq. (4) gives

$$\sum_i \sum_j a_{ij}^r (H_{kl,ij} - E_r\delta_{kl,ij}) = 0 \quad (5)$$

where $i,k = 0, 1, 2, \ldots, N_s$ and $j,l = 0, 1, 2, \ldots, N_b$.

The non-trivial solution of Eq. (5) are obtained from setting the secular determinant $|H_{kl,ij} - E_r\delta_{kl,ij}|$ to zero.

The matrix elements $H_{kl,ij}$ are readily obtained as algebraic expressions involving i,j,k,l and the potential parameters from existing tables in Ref. [16]. For the symmetric case, half of the eigenvalues, designated as $|\bullet\rangle_+$, have symmetric eigenfunctions about the $Q_s = 0$ axis, whereas the other half, designated as $|\bullet\rangle_-$, are antisymmetric about this axis. The $|\bullet\rangle_+$ eigenvalues were computed using even values of i,k and $|\bullet\rangle_-$ eigenvalues using odd values of i,k. Since, there is no symmetry about the $Q_b = 0$ axis, all allowed values of j,l were used. The main 30×20 matrix ($N_s = 29$ and $N_b = 19$) was diagonalized utilizing Microsoft FORTRAN Power Station V.1.

2.2. Test of convergence

Before interpreting the results, it is necessary to establish the reliability of the calculated quantities. In other words, we want to see that our results are fully converged with respect to the selection of harmonic force constants in the X and Y directions, the origin of the wave function expansion, and the size of the matrix.

Dependence of the energy levels on the harmonic basis set was examined and the results were invariant over a wide range of values chosen for the harmonic force constants and any particular number in that range was suitable for our study. Thus, a value of 300 N/m was employed for the harmonic stretching force constant (K_s) along the Q_s coordinate, and a value of 208 N/m was chosen for the harmonic bending force constant (K_b) along the Q_b coordinate.

Calculations also showed that the eigenvalues were independent of the choice of the origin of expansion located in large regions in the X and Y directions. Therefore, the origin of expansion was kept on the origin of the coordinate system.

With these choices for the harmonic force constants and the origin of expansion, the size effect of the matrix on the energy levels was then examined. After testing the convergence of energy levels on varying the number of basis functions in the Q_s and Q_b directions, we found that a 30×20 matrix (with $N_s = 29$ and $N_b = 19$) was big enough for the convergence of the lower energy levels pertinent to our subsequent discussions. Hence, this size of the matrix, 30×20 (with $N_s = 29$ and $N_b = 19$), was utilized for all calculations.

3. Results and discussion

3.1. Geometrical structure

All possible molecular structures of NO_2MA have been determined by Buemi and Zuccarello [17] at the B3LYP/6-311++G** level. We only considered the most stable *cis*-enol structure (Fig. 1a), the open *trans*-enol structure (Fig. 1b), and for comparison, the C_{2v} transition-state structure (Fig. 1c). The planarity of the molecule was verified by the microwave experimental data [8]. Detailed geometrical parameters of the *cis*-enol form of NO_2MA were already discussed before [7].

The calculated geometrical parameters of the hydrogen-bond systems along with the energy differences between the closed and open structures (E_{ct}) and the potential barrier heights from the lowest energy minima to the transition states of NO_2MA and MA (E_{BH}) are listed in Table 1. In addition, Table 1 also shows the calculated distance between the hydrogen-bond minima on the potential energy surface, ΔX, which is a very important parameter in proton tunneling and proton-transfer barrier height.

The data given in Table 1 indicate that substitution of the nitro group of NO_2MA by an α-hydrogen (*i.e.*, going from NO_2MA to MA) elongates the O···O and H···O distances, shortens the O–H distance, increases the barrier height for proton transfer (E_{BH}), and thus decreases the hydrogen-bond strength. Among all calculations at the B3LYP level, the hydrogen-bond parameters obtained with the 6-311++G** basis set, such as the O···O and O–H distances and ΔX, are in the best agreement with those obtained at the MP2/6-31G** level. Increasing the size of the basis sets used with B3LYP shifts the structural parameters towards those obtained at the MP2/6-31G** level. Refining the level of theory from MP2 to MP4 does not change the energy-related data (*e.g.*, E_{ct} and E_{BH}) much.

Moreover, we can further conclude that the hydrogen-bond system in NO_2MA deviates more from linearity compared with HFF, whose hydrogen-bond angle is quite close to a linear system (168.8–170.48°) [6]. This explains the higher barrier height for proton tunneling in NO_2MA than in HFF.

3.2. Potential surface of NO_2MA

Table 2 summarizes the $|0,0\rangle_+ \rightarrow |m,n\rangle_\pm$ transition frequencies calculated at the MP2/6-31G** and MP4/6-31G** levels. Here, m and n indicate the number of nodal lines of the wave functions along the stretching and bending directions, respectively. These results were obtained for a potential-energy cutoff of 2500 cm^{-1}, which is close to the ground-state energy with thermal correction at room temperature. This potential-energy cutoff was imposed on the potential energy of the hydrogen-atom motion. In other words, the amplitude of the hydrogen-atom motion at the ground state was restricted according to the potential-energy cutoff.

When the potential energy up to 2500 cm^{-1} was included in the two-dimensional nonlinear fit for calculating the potential parameters of Eq. (1), tunneling splittings of *ca.* 34.5 and 3.2 cm^{-1} were obtained for undeuterated and deuterated NO_2MA, respectively, in excellent agreement with previous microwave results, 35 ± 15 and 3.0 ± 0.02 cm^{-1} [8]. According to Table 2, the calculated ν_{OH}/ν_{OD} and δ_{OH}/δ_{OD} are *ca.* 2900/2100 and 1380/970 cm^{-1}, respectively. Previously reported ν_{OH} and ν_{OD} at about 2880 and 2100 cm^{-1} [7], respectively, are in excellent agreement with our latest theoretical results. In the study of the vibrational spectra of NO_2MA, we observed a weak and broad band near 1382 cm^{-1} [7], which upon deuteration disappears and two weak bands appear around 894 and 1061 cm^{-1} (with an average position at 977.5 cm^{-1}). The latter two weak bands are mainly δ_{OD}. Therefore, the observed O–H/O–D in-plane bending mode is also in excellent agreement with our latest theoretical predictions depicted in Table 2.

The corresponding barrier height for proton tunneling in NO_2MA, with respect to the midpoint between the two hydrogen-bond minima, is 46.4 kJ/mol, which is slightly lower than the corresponding value for MA (54.0–56.5 kJ/mol) [5] and is significantly higher than that for HFF (26.5–27.2 kJ/mol) [6]. This barrier height is considerably higher than that in the potential energy surface of fully optimized structures: $E_{BH} \approx 11$ kJ/mol (see Table 1), which is greatly underestimated by a factor of 4. Otherwise, we would expect a proton tunneling frequency of several orders of magnitude higher than that obtained experimentally. On the other hand, such a gross underestimation of the proton-transfer barrier height from the fully optimized potential energy surface is not completely unexpected. The much higher frequency of the O–H stretching mode directly involved in the hydrogen-bond motion makes it very hard for other structural parameters (except for the O–H bond distance and COH bond angle) to synchronize with the fast movement of the O–H bond. Therefore, to a good approximation, all other structural parameters not directly involved in the hydrogen-bond motion should stay at their average equilibrium positions. This justifies the procedure adopted in this work.

Table 1
Comparison of hydrogen-bond geometrical parameters of NO_2MA and MA (numbers in parentheses).

Theory	O···O[a]	O–H[a]	H···O[a]	∠OHO[b]	E_{ct}[c]	E_{BH}[d]	ΔX[e]
MP2/6-G**	2.577 (2.591)	0.999 (0.995)	1.679 (1.695)	147.4 (147.7)	50.5 (58.6)	13.6 (15.2)	0.708 (0.730)
MP4/6-1G**[f]	2.577 (2.591)	0.999 (0.995)	1.679 (1.695)	147.4 (147.7)	48.4 (55.6)	10.9 (16.5)	0.708 (0.730)
B3LYP/6-1G**	2.533 (2.553)	1.015 (1.008)	1.612 (1.640)	148.4 (148.5)	59.8 (62.8)	7.1 (9.2)	0.620 (0.658)
B3LYP/6-1G*	2.570 (2.590)	1.011 (1.005)	1.665 (1.690)	146.6 (146.9)	62.6 (59.0)	12.4 (14.4)	0.682 (0.714)
B3LYP/6-11G**	2.557 (2.581)	1.004 (0.998)	1.657 (1.687)	146.8 (146.8)	55.4 (58.1)	11.0 (13.2)	0.680 (0.719)
B3LYP/6-11++G**	2.559 (2.587)	1.004 (0.997)	1.664 (1.700)	146.2 (145.9)	53.4 (54.1)	11.1 (13.4)	0.689 (0.735)
Experiment [16]	(2.553)	(0.969)	(1.680)	(147.6)			

[a] Atomic distance (in Å).
[b] Bond angle (in °).
[c] Energy difference (in kJ/mol) between the closed *cis*-enol and the open *trans*-enol forms.
[d] Potential barrier height (in kJ/mol) from the lowest energy minimum (the closed *cis*-enol form) to the C_{2v} (transition state) structure.
[e] Distance (in Å) between the two hydrogen-bond minima.
[f] MP4/6-1G** calculations were based on the MP2/6-1G** optimized geometries.

Table 2
Theoretical and experimental transition frequencies (in cm^{-1}) for undeuterated and deuterated NO_2MA.[a]

	$\|0,0\rangle_+ \rightarrow \|0,0\rangle_-$	$\|0,0\rangle_- \rightarrow \|0,1\rangle_+$	$\|0,0\rangle_+ \rightarrow \|0,1\rangle_-$	$\|0,0\rangle_- \rightarrow \|1,0\rangle_+$	$\|0,0\rangle_+ \rightarrow \|1,0\rangle_-$	$\|0,0\rangle_+ \rightarrow \|1,1\rangle_-$	$\|0,0\rangle_- \rightarrow \|1,1\rangle_+$
MP2	35.5, 3.4	1114, 930	1399, 978	2658, 2070	2904, 2104	4425, 3133	3459, 2934
MP4[b]	33.5, 3.1	1092, 913	1371, 959	2657, 2069	2893, 2103	4399, 3111	3411, 2913
Exp.	35 ± 15,[c] 3.00 ± 0.02[c]		1382,[d] 977.5[d,e]		2880,[d] 2100[d]		

[a] In each column, first and second numbers are undeuterated and deuterated data, respectively.
[b] MP4/6-1G** calculations were based on the MP2/6-1G** optimized geometries.
[c] From Ref. [8].
[d] From Ref. [7].
[e] Averaged δ_{OD} frequency.

Finally, despite taking into account all structural relaxation effects between the *cis*-enol and the *trans*-enol forms of NO_2MA, E_{ct} should serve as a rough guide to the hydrogen-bond strength. The data shown in Table 1 suggest that the hydrogen-bond strength in NO_2MA is probably higher than 50 kJ/mol.

4. Conclusion

A simple two-dimensional potential function was applied to calculate the hydrogen-bond transition frequencies in NO_2MA. In this method, *ab initio* programs were used to generate a two-dimensional potential energy surface, which correctly predicted the equilibrium molecular geometries. This potential function, which couples the O–H stretching to the in-plane bending motion, was then employed to calculate the O–H/O–D vibrational energy levels. For NO_2MA, this method predicted the proton tunneling, O–H/O–D stretching and in-plane bending frequencies all in excellent agreement with experimental data. A proton-transfer barrier height of 46.4 kJ/mol was estimated for the hydrogen-bond system in NO_2MA.

Acknowledgements

Y.A.W. gratefully acknowledges the financial support from the Natural Sciences and Engineering Research Council (NSERC) of Canada. WestGrid and C-HORSE have partially provided the necessary computational resources.

References

[1] W.W. Cleland, Biochemistry 31 (1992) 317.
[2] W.W. Cleland, M.M. Kreevoy, Science 264 (1994) 1887.
[3] C.B. Aakeröy, K.R. Seddon, Chem. Soc. Rev. 22 (1993) 397.
[4] A.U. Khan, M. Kasha, Proc. Natl. Acad. Sci. USA 80 (1983) 1767.
[5] S.F. Tayyari, M. Zahedi-Tabrizi, F. Tayyari, F. Milani-Nejad, J. Mol. Struct. (Theochem) 637 (2003) 171.
[6] S.F. Tayyari, M. Zahedi-Tabrizi, H. Rahemi, H.A. Mirshahi, J.S. Emampour, M. Rajabi, F. Milani-Nejad, J. Mol. Struct. (Theochem) 730 (2005) 17.
[7] S.F. Tayyari, Z. Moosavi-Tekyeh, M. Zahedi-Tabrizi, J.S. Emampour, H. Rahemi, M. Hassanpour, J. Mol. Struct. 782 (2006) 191.
[8] W. Caminati, J. Chem. Soc., Faraday Trans. 2 (78) (1982) 825.
[9] M.J. Frisch et al., Gaussian 03, Revision D.01, Gaussian, Inc., Wallingford CT, 2004.
[10] Fortran code of DBMIN2 is available from the authors upon request. Contact sftayyari@yahoo.com.
[11] Genplot package, Computer Graphic Service, Cornell University, Ithaca, New York, 1990.
[12] J.W. Bevan, MSc thesis, University of Surrey, UK, 1969.
[13] I. Matanović, N. Došlić, J. Phys. Chem. A 109 (2005) 4185.
[14] J.A. Ibers, J. Chem. Phys. 41 (1964) 25.
[15] T.R. Sing, J.L. Wood, J. Chem. Phys. 48 (1968) 4567.
[16] E.B. Wilson, J.C. Decieus, P.C. Cross, Molecular Vibrations, McGraw-Hill, New York, 1955 (Appendix III).
[17] G. Buemi, F. Zuccarello, Chem. Phys. 306 (2004) 115.